H-SAF

VSA Programme

HSAF_ CDOP2_VS14_03

Improvements on the PR-OBS-6 H-SAF precipitation product using multispectral markers from geostationary satellite data

Final report

Index

Table of Figures

1. Scope of the document

The aim of this document is to describe the visiting scientist activity about the development of a new algorithm for the convective objects detection in support to the H15 product.

The algorithm shall be able to work on the Meteosat Second Generation (MSG) satellite working area within the MSG 15 minutes timeliness.

2. Introduction

Mesoscale Convective Systems (MCSs) are of great importance due to their direct impact on human life and property. They produce severe weather conditions such as heavy rain, hail, strong winds, tornadoes, lightning, and flooding that can significantly impact human activities. Their horizontal dimensions extend a few hundred kilometres in one direction, reaching many thousand kilometres in some cases ([8]; [9]; [13]) and their lifecycles range approximately from a few hours to as long as 1–2 days ([10]; [11],[12])

Ground-based weather radars are commonly used to provide accurate information about the presence, the shape and the structure of MCSs.

The use of modern geostationary meteorological satellites with their fine time (15 min) and space (3 km at the sub-satellite point) sampling and large geographical coverage has become an excellent alternative way to face the uncertainness and the restrictions of many numerical models and radars in MCS forecasting

In general a short-range (0–12 h) MCS forecasting procedure based on satellite or radar data can be implemented in three main stages ([14]): early warning of convection, detection of convective cells and forecasting their movement and evolution.

Product PR-OBS-6 (Blended SEVIRI Convection area/ LEO MW Convective Precipitation) is based on the SEVIRI instrument on board the Meteosat Second Generation satellites and acts on the first two stages in order to provide an early warning and a detection of the convective objects.

An objective analysis of the equivalent blackbody temperatures (TBB) is implemented to detect the convective structures of cloudy areas, by means of NEFODINA, an automatic tool running at COMet dedicated to nowcasting applications. A map of convective clouds is performed to combine precipitation fields from MW instrument.

The main objective of the proposal is to improve the performance of the PR-OBS-6 product by means of the development of a novel algorithm for the detection of the convection.

3. The Nefodina algorithm

The NEFODINA (DYNAmic NEFOanalisys) [15] product has been developed by Italian Air Force Met Service (IAFMS) to estimate thunderstorms presence and intensity using only geostationary satellite data. More precisely using a multichannel approach it provides information on convective nuclei inside cloudy systems (from mesoscale down to single cell thunderstorm). This is an important information for the forecasters to diagnose the convective activity, evaluate its severity and its potential development. Moreover, NEFODINA determines also the Convective Objects' (COs) life phase (developing/dissolving phase).

During its life, a cell passes different phases: in particular we can speak about a cumulus stage, a growing or mature phase and finally a dissipating stage. During the growing phase, when the lightning density shows a

maximum, the most intensive weather activities, heavy rainfall, thunderstorms and hail showers occurs and frequently cause significant damage.

NEFODINA software runs at IAFMS since 1996 and every day its performance and reliability is tested by Italian forecaster. Initially based only on 10.8 μm IR channel, studies on the correlation between the electric activity measured by the Lightning Network (LN) of the IAFMS and convective systems features detectable by MSG pointed out the necessity to use both infrared (IR) window and water vapour absorption bands to achieve a good operational detection and tracking of convective objects. The use of MSG water vapour (WV) channels appears very efficient not only for separating high level cloudiness from clear sky and low clouds but also for estimating the horizontal distribution of the WV amount in the middle-high troposphere.

4. The Nefodina2 algorithm

The main purpose of the Nefodina2 algorithm is able to detect and track convective events using the Meteosat Second Generation (MSG) data as unique data source.

The algorithm follows an Object Oriented (OO) approach in order to better handle the amount of data and to apply standard techniques for the properties definition of the detected objects.

The components used to characterise the convective objects are the following:

- Detector
- Tracker

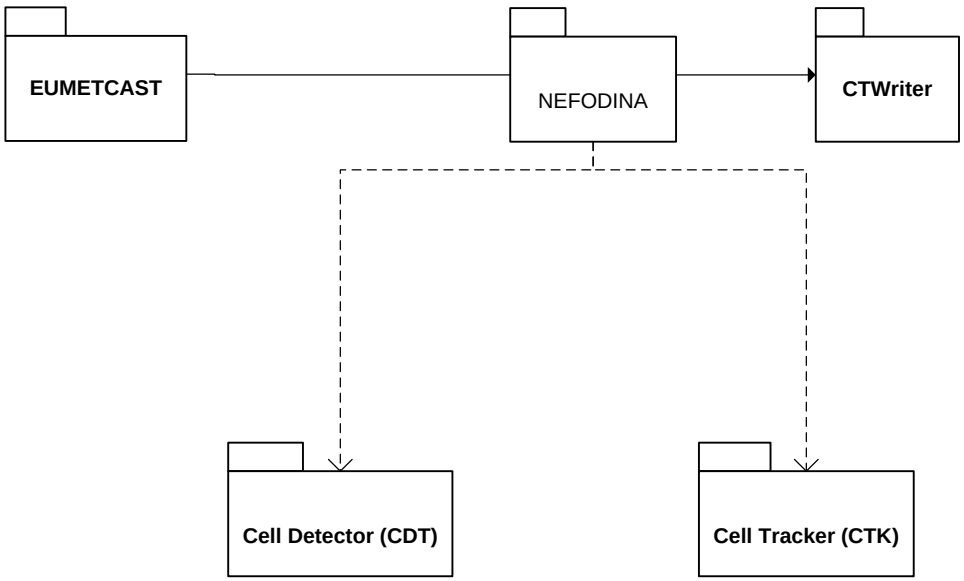

Figure 1: Components view of the algorithm

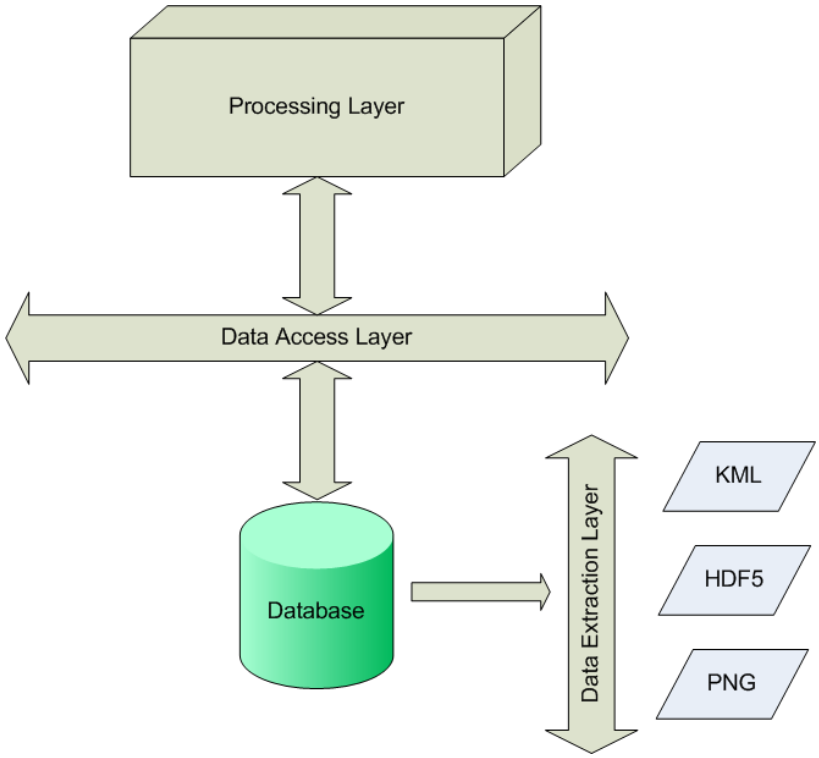

Figure 2: Layers view of the algorithm

The **Detector** (CDT) applies a multispectral approach using two MSG channels for the detection of the convective areas, more specifically it apply the difference between the 6.2 µm and the 10.8 µm channels ([1]) in order to extract the top of the convective clouds.

After this step, the algorithm applies the K-means algorithm in order to identify the colder pixels on the 10.8 µm channel.

The k-means clustering is a method of vector quantization, originally from signal processing, that is popular for cluster analysis in data mining. K-means clustering aims to partition n observations into k clusters in which each observation belongs to the cluster with the nearest mean, serving as a prototype of the cluster.

Applied to the Nefodina2, the clustering algorithm makes a partition of the convective pixels, identified at the previous stage, and it retains only the ones belonging to the colder class.

In this way it is possible to avoid the use of fixed thresholds and the algorithm could be applied to the full disk area.

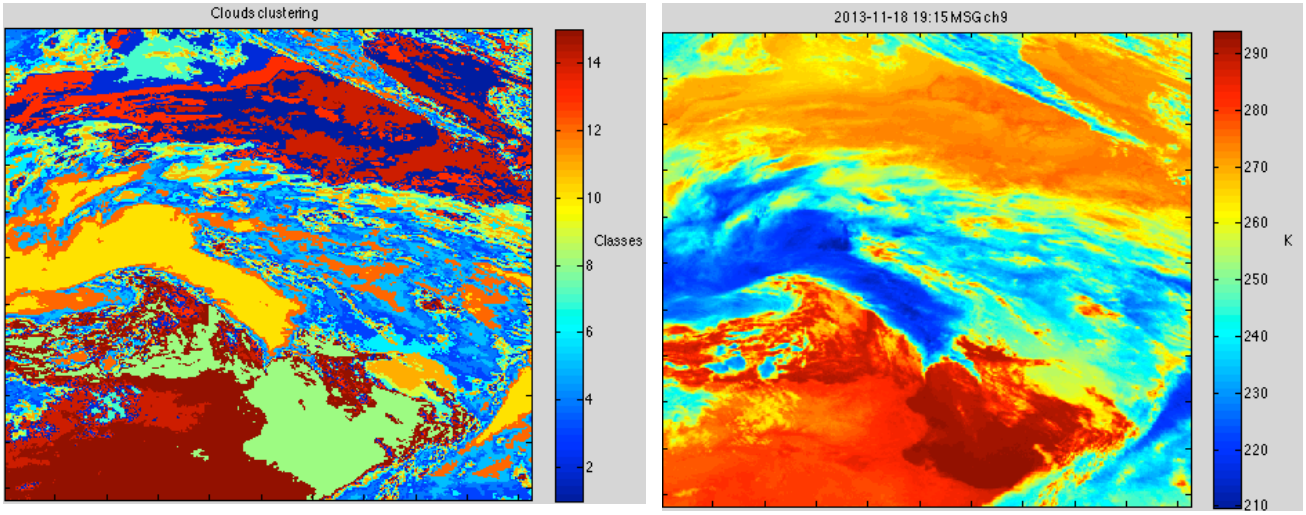

Figure 3: MSG image segmantation using the K-means algorithm

The outputs of the previous steps are two binary maps regarding the convective object characterization at the upper layers of the atmosphere.

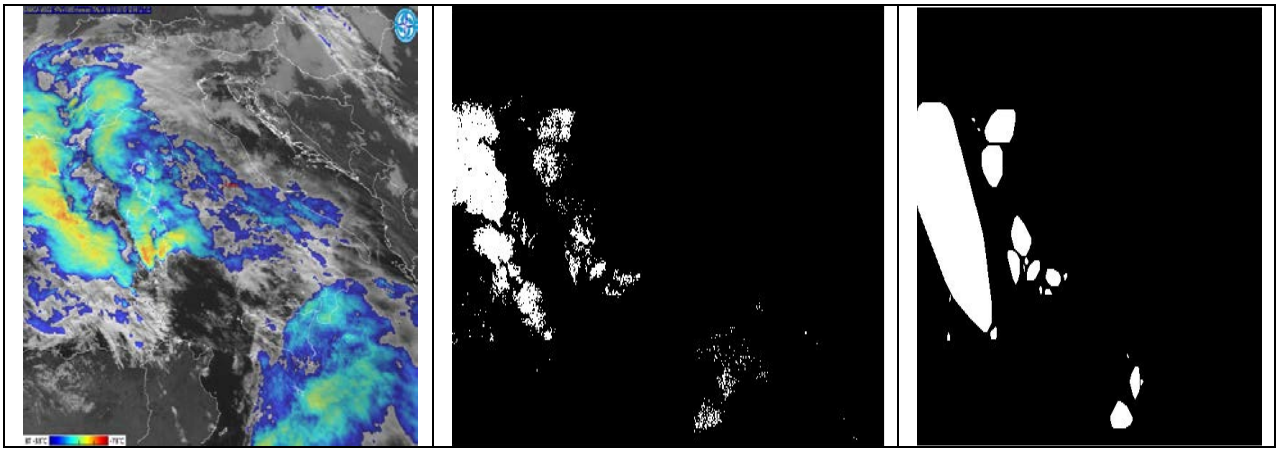

Figure 4: Nefodina2 detection steps. On the left the MSG input image. The center image shows the binary image deriving from the difference between the channel 5 and 9. The right image shows the object extraction by using a clustering algorithm.

The Tracker (CTK) makes a temporal correlation between the objects detected at the previous time slots. The correlation is done by intersecting the objects at time $t-1$ with the objects detected at time t. If the intersection is not empty, then the objects are related through a parent-child relationship.

CTK is also responsible to assign the phase to each convective object based on the differences of the object properties (areas) between two consecutive MSG slots.

Summarizing the main features of the Nedofina2 algorithm are the following:

- MSG as data source
- Detection of the convective objects (cloud tops and nuclei)
- Tracking of the detected objects
- Cells lifecycle monitoring

5. Methods and Techniques

In this section the techniques and the methods used to validate and compare the model output are presented.

5.1.The Model Evaluation Tool (MET)

The Model Evaluation Tool (MET) is a set of verification tools developed by the Developmental Testbed Center (DTC) for use by the numerical weather prediction community – and especially users and developers of the Weather Research and Forecasting (WRF) model – to help them assess and evaluate the performance of numerical weather predictions.

The primary goal of MET development is to provide a state-of-the-art verification package to the NWP community. By "state-of-the-art" we mean that MET will incorporate newly developed and advanced verification methodologies, including new methods for diagnostic and spatial verification and new techniques provided by the verification and modeling communities.

Several tools are part of the MET package and the MODE tool has been chosen for the validation of the Nefodina2 algorithm.

The MODE (Method for Object-based Diagnostic Evaluation) tool uses gridded fields as observational datasets. MODE applies the object-based spatial verification technique described in [16].

5.2.ATDNet

The Arrival Time Difference (ATD) Thunderstorm detection system is a low-cost innovation that has grown out of a requirement placed on the Met Office to locate thunderstorms for general weather prediction [public safety], the national Electricity supply Grid and Defense operations . The outputs find many applications, for instance, to verify occasions of very intense rainfall detected by the weather radar network.

The ATD system works by detecting the vertical component of the electromagnetic field generated by a lightning discharge at a narrow band frequency in the range 10 to 14 kHz. Strong electromagnetic emissions at these frequencies are caused by rapid neutralisation of charge in the lowest few hundred meters of cloud to ground (C-G) strokes. Atmospheric attenuation at these frequencies is very low and the electromagnetic discharge (SFERIC) can propagate over thousands of kilometers along the earth-atmosphere wave guide. ATDNET outstations, Fourier analyze the SFERIC wave and the waves from different outstations are correlated in the central processor to produce the time difference used for flash location. 3 pairs of time differences are required to obtain a location, but it is preferable to have at least 4 if possible, to guard against error in one of the individual time differences and solve ambiguity location.

The ATD system is not very sensitive to cloud to cloud strokes especially at long range from the sensors, since it primarily senses SFERICS polarized in the vertical. Details of the system are presented in [17] with some ideas about extending the system for global coverage. Detection characteristics of the existing ATDNET were first presented in [18]. The existing system has used several New Outstation [NOS] to maintain and improve its operations since 2004, so the Met Office is quite confident about the stability of operation of the NOS sensing systems, including software.

However, a completely new ATDNET system became operational in December 2006, using a larger number of NOS than possible previously. A new flash location processors feeds locations into a Logical Data Store and then into a Product Generation System.

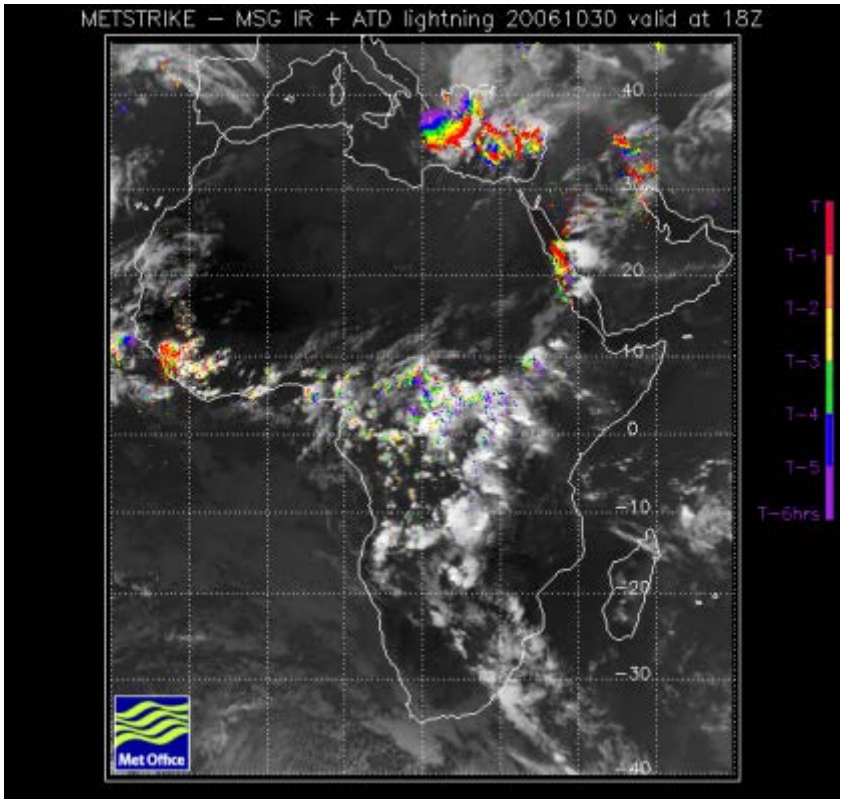

Figure 5: Current ATD superimposed on Meteosat MSG cloud picture – a possible product for supply to Africa with ATDNET. Here the latest observations are in red and the observations 6 hours earlier are in purple.

5.3.Lightning data usage

The ATDNET lightning data are used as ground truth in order to match the convective areas with the objects detected by the Nefodina2 algorithm. The lightning data are temporally filtered by selecting the strokes around the MSG timeslot based on the latitude.

After this temporal filtering, the strokes field is placed on the same grid as well as the detected objects in order to make a comparison between the two fields. In order to make this, the data are packed into a NetCDF file using the CF conventions ([19]).

Finally the two fields are compared using the MODE tool provided by the MET framework.

6. The RDT algorithm

The RDT, Rapid Development Thunderstorm, product has been developed by Meteo-France in the framework of the EUMETSAT SAF in support to Nowcasting. Using mainly geostationary satellite data, it provides information on clouds related to significant convective systems, from meso-alpha scale (200 to 2000 km) down to smaller scales (few pixels). It is provided to users in the form of numerical data stored in a BUFR format file.

The objectives of RDT are twofold:

- The identification, monitoring and tracking of intense convective system clouds
- The detection of rapidly developing convective cells

The object-oriented approach underlying the RDT product allows to add value to the satellite image by characterizing convective, spatially consistent, entities through various parameters of interest to the

forecaster: motion vector, cooling and expansion rate, cloud top height… and their time series. It supports easy and meaningful downstream data fusion (surface observations, NWP fields, radar data...).

7. Results

Some case studies have been selected to validate the Nedofina+ product. The validation process involves the use of the MET framework and the MODE tool in particular in order to apply an object oriented approach for the validation. The tool compares two fields, the lightning and the Nefodina2 fields, and identifies the objects inside them.

A likelihood function is applied to each pair of objects belonging to each field and the paired objects are matched. Figure 5 shows the graphical output of the MODE tool.

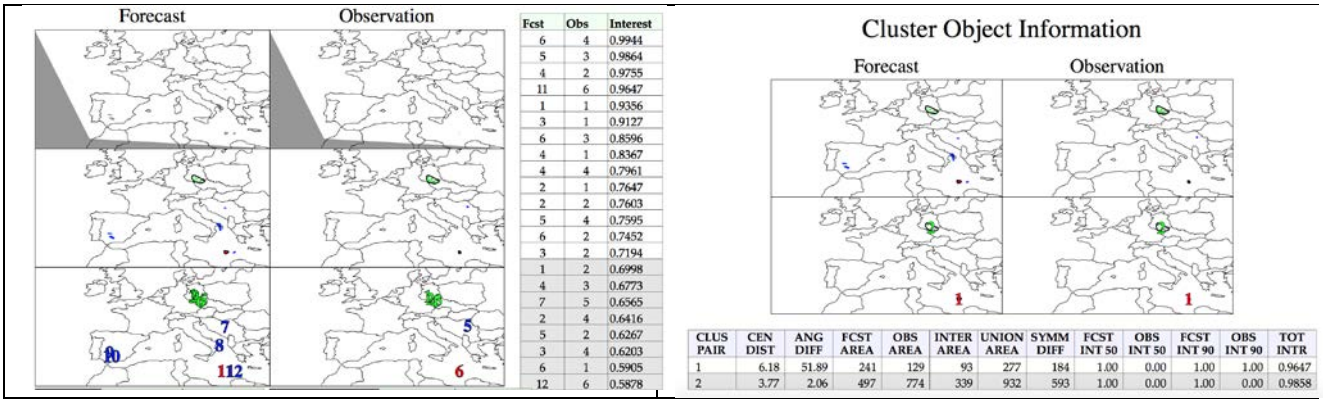

Figure 6. Postscript MODE output: the left side figure shows the objects identification process and the likelihood function values for each pair. The right side figure show the matched labelled objects with some statistics.

At this step it is possible to compute some statistical scores in order to measure the goodness of the model under assessment. The chosen scores are Probability of detection (POD) and False alarm ratio (FAR).

Forecast	**Observation**		**Total**
	O=1 (e.g. "Yes")	O=0 (e.g. "No")	
f = 1 (e.g., "Yes")	n_{11}	n_{10}	$n1. = n_{11} + n_{10}$
f = 0 (e.g., "No")	n_{01}	n_{10}	$n0.= n_{01} + n_{00}$
Total	$n_{.1} = n_{11} + n_{01}$	$n_{.0} = n_{10} + n_{00}$	$T = n_{11} + n_{10} + n_{01} + n_{00}$

Table 1: 2x2 contingency table in terms of counts. The n_{ij} values in the table represent the counts in each forecast-observation category, where *i* represents the forecast and *j* represents the observations. The "." symbols in the total cells represent sums across categories.

The counts, n_{11}, n_{10}, n_{01}, and n_{00}, are sometimes called the "Hits", "False alarms", "Misses", and "Correct rejections", respectively.

POD is defined as

$$POD = \frac{n_{11}}{n_{11} + n_{01}} = \frac{n_{11}}{n_{.1}}$$

It is the fraction of events that were correctly forecasted to occur.

FAR is defined as

$$FAR = \frac{n_{10}}{n_{11} + n_{10}} = \frac{n_{10}}{n_{1.}}$$

It is the proportion of forecasts of the event occurring for which the event did not occur.

7.1. 2013-11-18 severe storm at Sardinia

On 18th November 2013 a severe storm hit Sardinia causing damages, dead and injured people. The media reports that at least 18 people died when 3 m (10 ft) high floods swept through parts of the island. The worst affected area was in and around the city of Olbia where much of the city was said to have been flooded.

Figure 7 shows the channel 9 brightness temperature at 14:00 UTC. It is possible to see very high clouds over Sardinia.

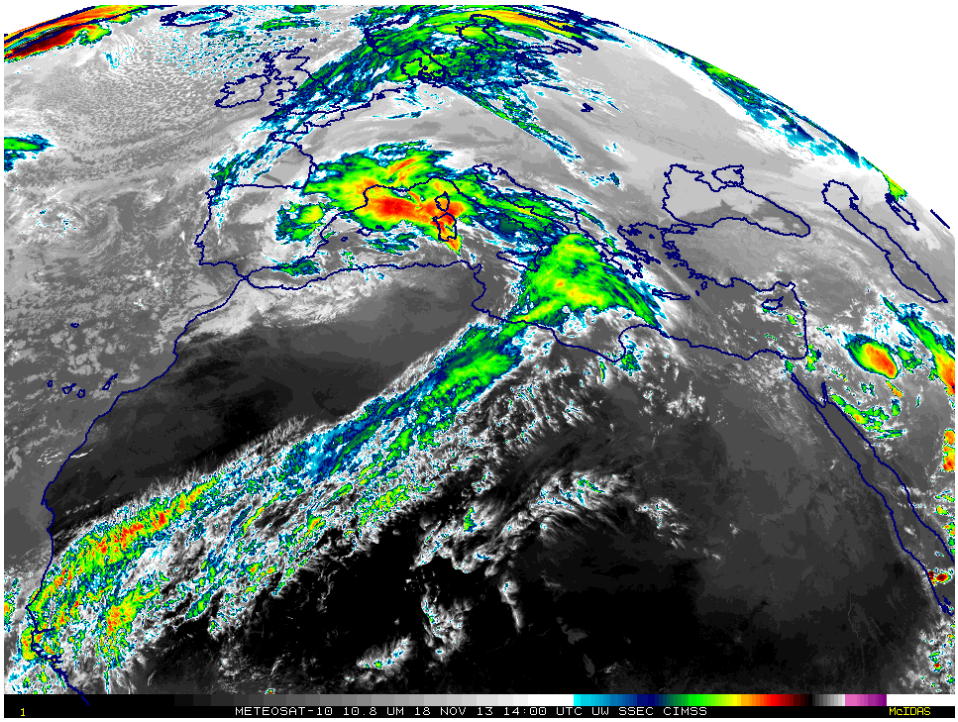

Figure 7: MSG 10.8 µm infrared channel for the Sardinia case study at 14:00 UTC

Figure 8 shows the MSG water vapor channel at 6.2 µm and it is possible to note the presence of moisture at very high altitude (above 16KM).

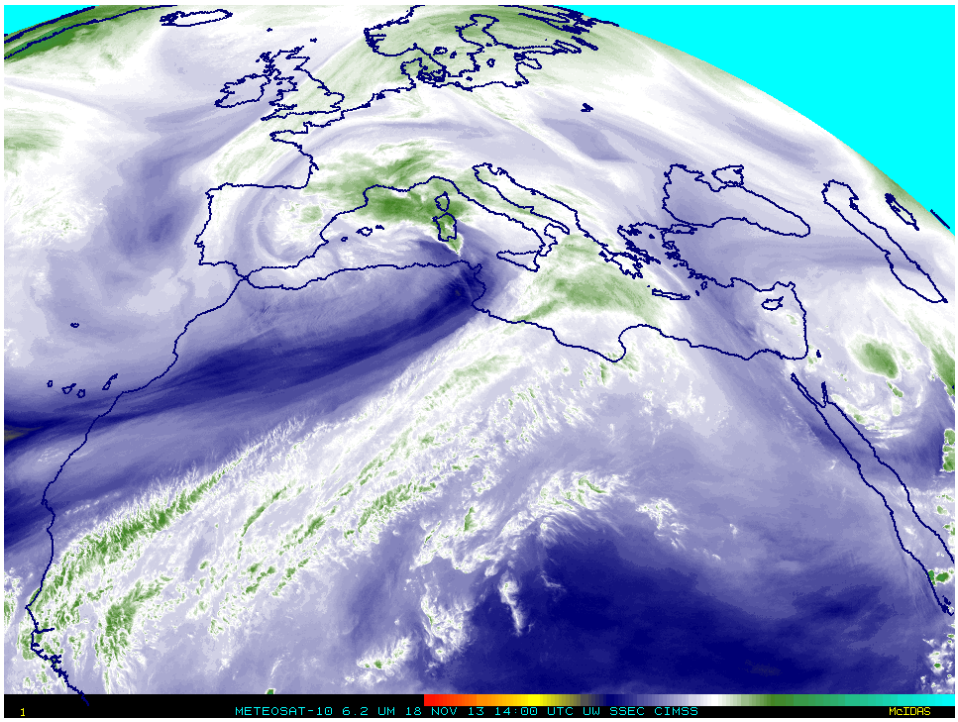

Figure 8: Meteosat-10 6.2 µm water vapor channel for the Sardinia case study at 14:00 UTC

7.2. Event statistics

In this section some event statistics are depicted. More in detail the number of strokes at MSG time slots and the stroke density has showed in order to characterize better the event.

The validation area is depicted by Figure 6:

Figure 9: Validation area for the event over Sardinia

Figure 10 and Figure 11 show the statistics of the event:

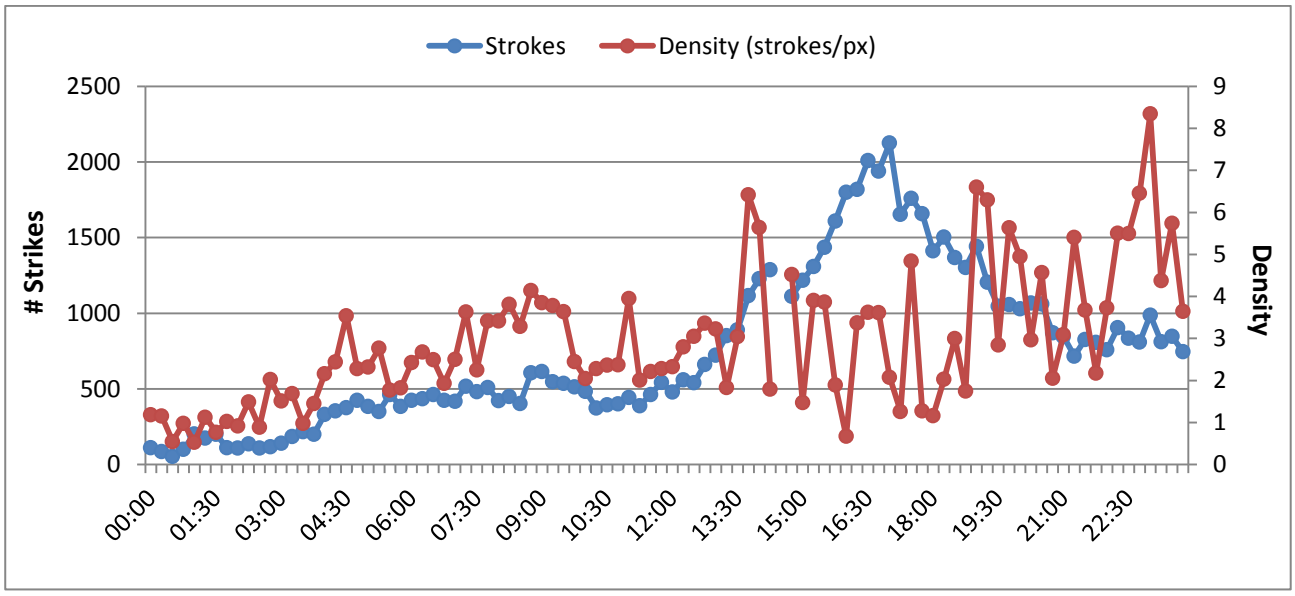

Figure 10: Number of strokes and strokes density related to the event. Note the increasing of the total strokes starting from the 15:00 UTC

Figure 10 shows the strokes trend during the whole day. A spike no density appeared to predict the event at 13:30 UTC, while the number of strokes peaked at 16:30 UTC.

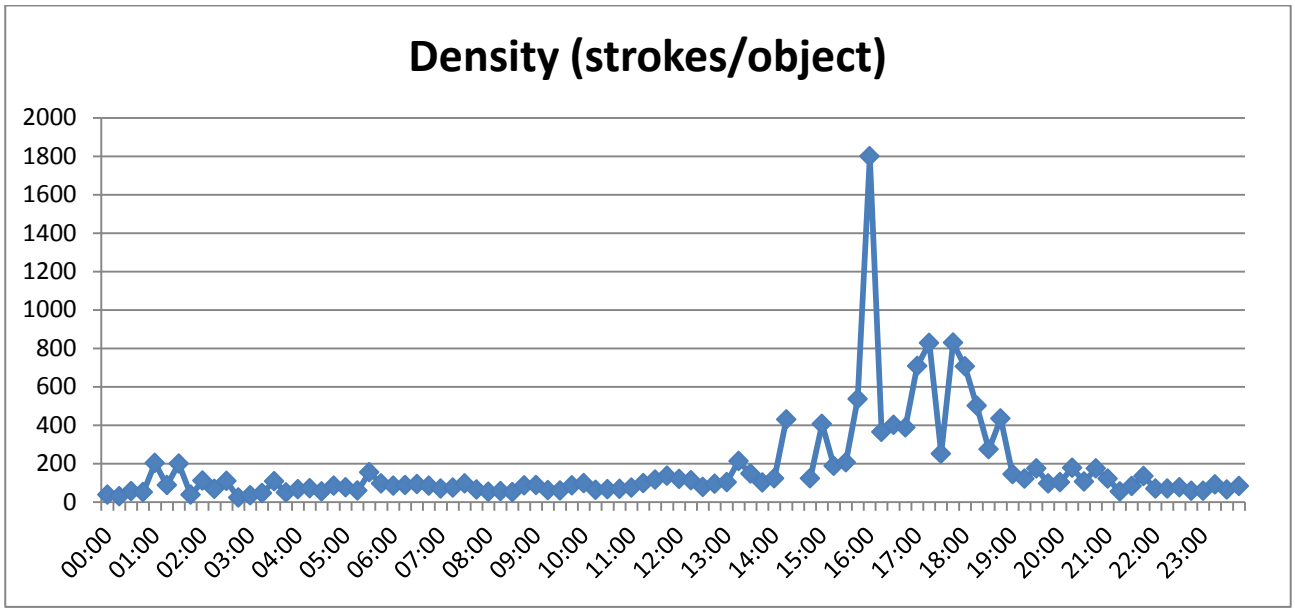

Figure 11: Density (strokes per object) about the event.

The event dynamics is well depicted by Figure 11. Note the density spike at about 16:00 UTC, when the event reached the maximum of its power.

7.3.Results

In this section the validation results on the case study are presented. The performance are presented as scores graph and the scores are computed against the total number of strokes occurred 10 minutes after and 5 minutes before the MSG time slot to take into account the scanning delay at these latitudes.

Figure 12 shows the scores computed over the validation area using the MODE tool. It is important to note the POD trend. It starts to increase as the increasing of the number of strokes and reaches the peak at about 15:00 UTC.

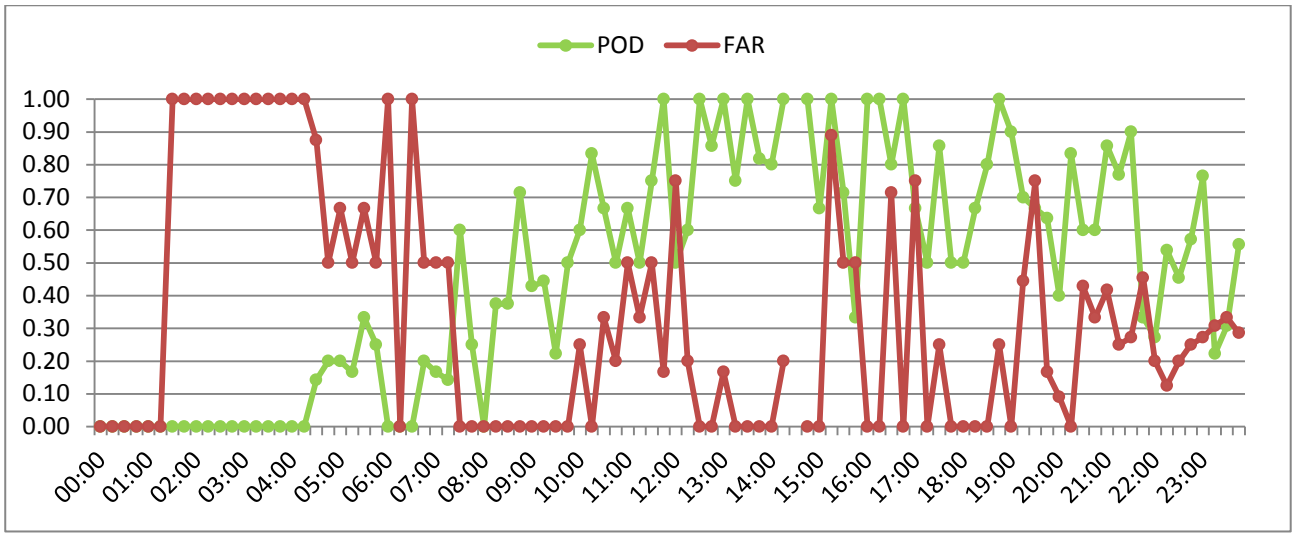

Figure 12: Nefodina2 scores computed for the case study

Figure 13 shows the RDT scores computed over the validation area. The POD seems to be almost steady from the morning. It is important to note that this behavior of the model because it is weakly coupled with the strokes. Probably it is due to the use of the NWP data as input.

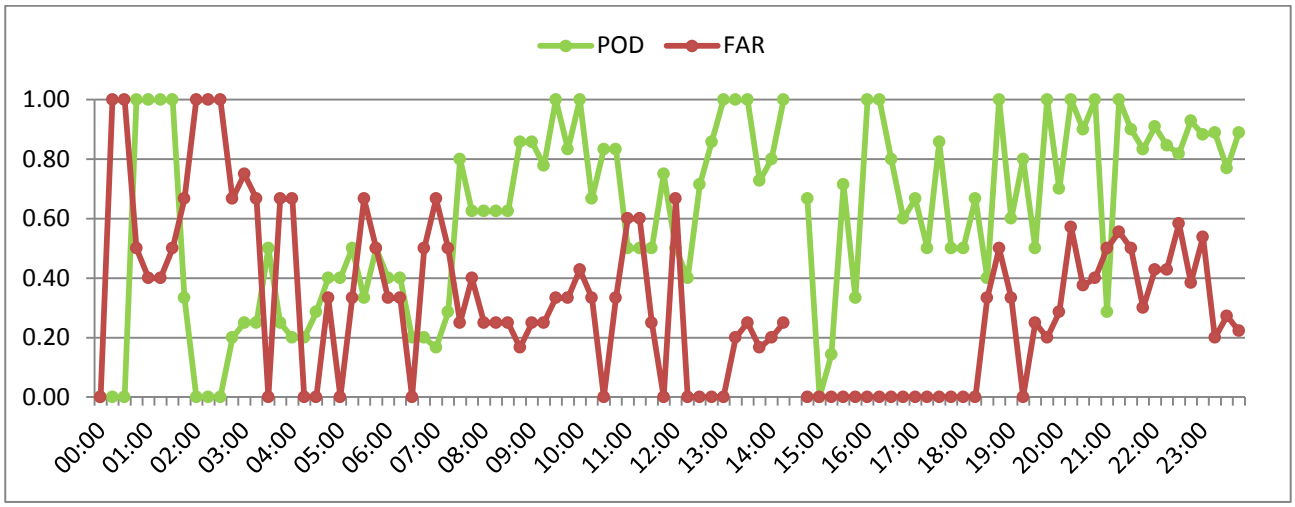

Figure 13: RDT scores computed for the case study

Figure 14 shows the POD trend of the Nefodina2 and the RDT models. It is possible to note that the Nefodina2 score is very sensitive to the number of strokes while the RDT POD is much more constant over the whole validation period. By the way, during the hours of the event the two models perform very well and the POD of both is above 0.6, with a better value for Nefodina2.

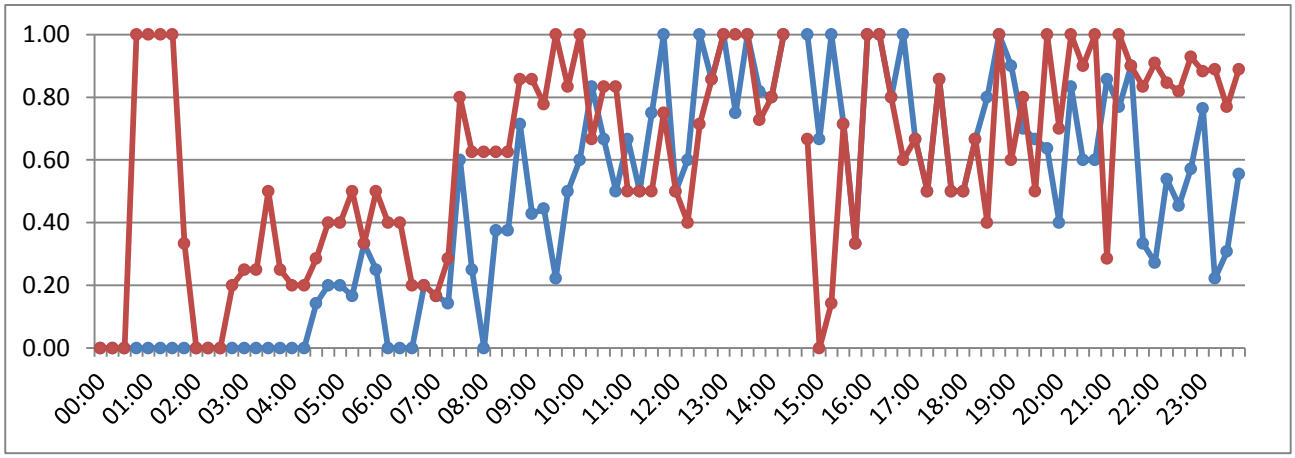

Figure 14: POD scores comparison between Nefodina2 and RDT. In red the Nefodina2 POD and in blue the RDT POD.

Figure 15 shows the comparison between the FAR scores of Nefodina2 and RDT. An overall lower RDT FAR is evident due to the use of the NWP and lightning data, while the Nefodina FAR decreases during the event period.

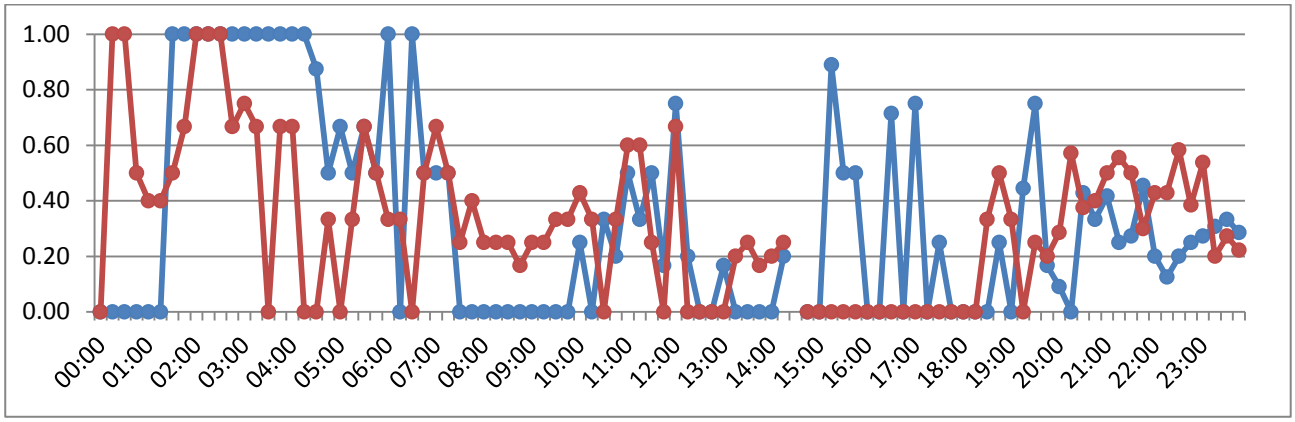

Figure 15: FAR scores comparison between Nefodina2 and RDT. In red the Nefodina2 FAR and in blue the RDT FAR.

8. South Africa case studies

8.1. The South African Lightning Detection Network (SALDN)

The SALDN sensors detect electromagnetic signals emitted by lightning discharges. Low frequency waves can propagate along the ground, called ground waves, and also through the atmosphere, called sky waves. Each sky wave is given a number according to how many times it has been reflected by the ionosphere.

The first sky wave is reflected once by the ionosphere, the second twice, etc. The SALDN sensors operate at very low frequency and low frequency ranges. This range of operation is to ensure that the sensors detect only the ground waves and not the sky waves and thus cloud-to-ground lightning flashes. Each lightning discharge produces a wave pulse signature that is unique. These signatures are analysed to determine the type of stroke. The SALDN sensors detect electromagnetic waves by means of a combination of magnetic direction finding and time of arrival methods.

The magnetic direction finding method determines the angle from true north between the sensor and lightning stroke whilst the time of arrival method pinpoints the possible location of a lightning stroke based

on the different arrival times between the sensors in order to use the parabolic and circular method to determine the intersection point of the stroke.

When the time of arrival or the magnetic direction finding method is used individually, three or more sensors are needed, whilst the combined technology as used by the SALDN requires at least two sensors to detect lightning.

In the development of the lightning climatology, only cloud-to-ground lightning flashes were considered because the SALDN detects this type of lightning.

The lightning sensors installed by the SAWS are distributed throughout the country (Figure 18).

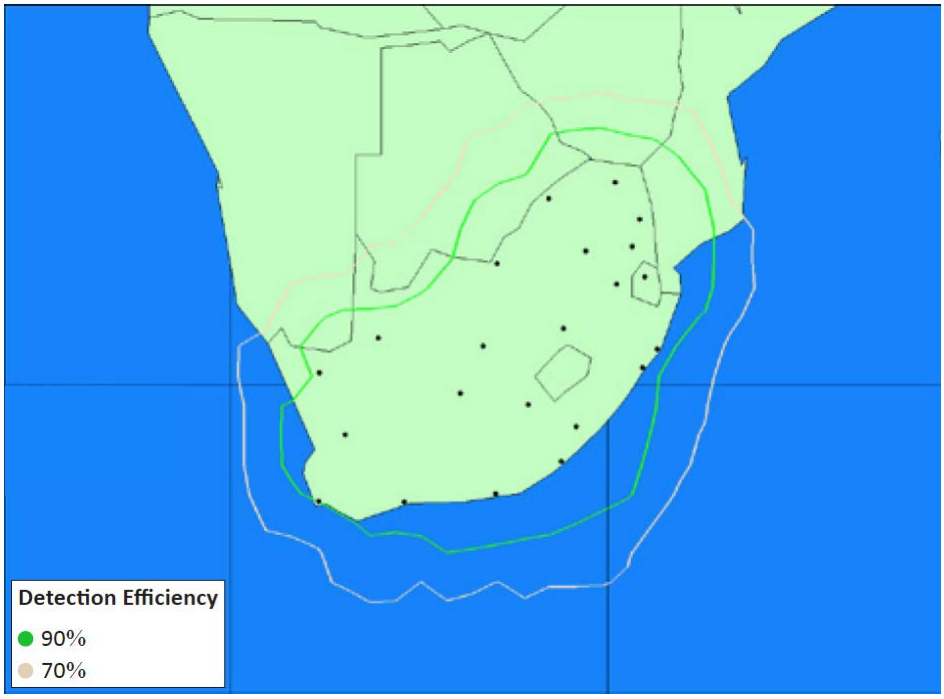

Figure 16: Map indicating the positions of the South African Weather Service lightning detection network sensors distributed throughout South Africa together with the detection efficiency rings at the present time.

More information about the SALDN can be found in [20].

8.2. 8th December 2014: South Africa case study

On 8th December 2014 several thunderstorms developed at Eastern South Africa in the afternoon. About 40000 strokes were encountered from 12:00 UTC to 18:00 UTC.

Figure 16 is a MSG RGB image which shows the weather situation over South Africa at 15:00 UTC. It is possible to see the development of several severe thunderstorms at Eastern.

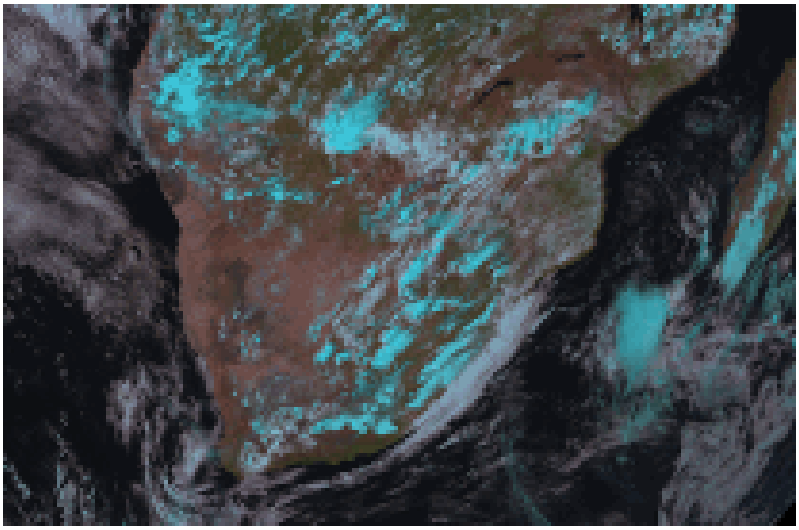

Figure 17: Thunderstorms developments at Eastern of South Africa on 2014-12-08 15:00 UTC

The synoptic situation is presented by Figure 17. A lower pressure over Botswana brings moisture from the ocean creating the conditions for thunderstorms development.

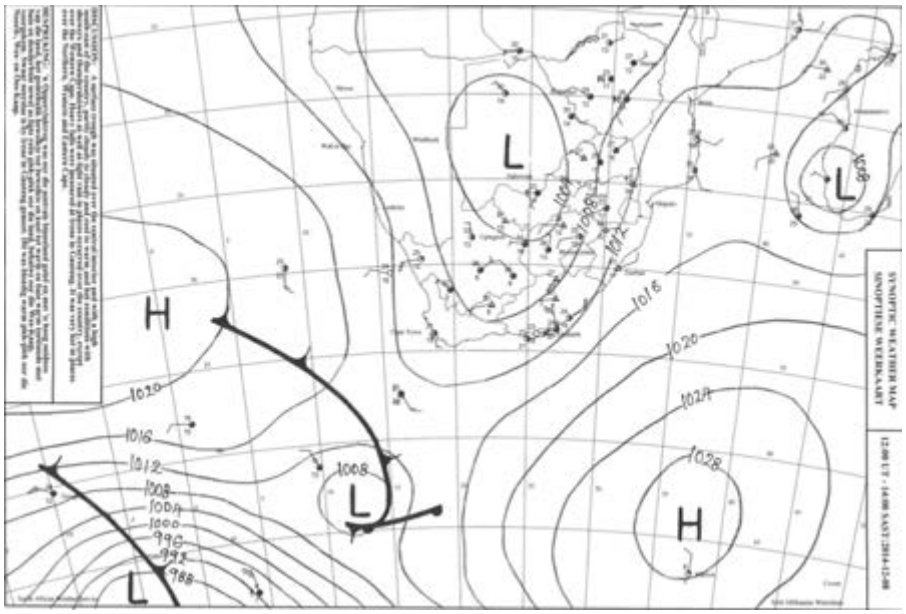

Figure 18: Synoptic chart relative to the 2014-12-08 at South Africa

8.3.Event statistics

In this section some statistics about the event are presented in order to describe better the weather situation of the case study.

Figure 18 shows the validation area at South Africa which is compliant with the lightning detection network green area shown in Figure 18.

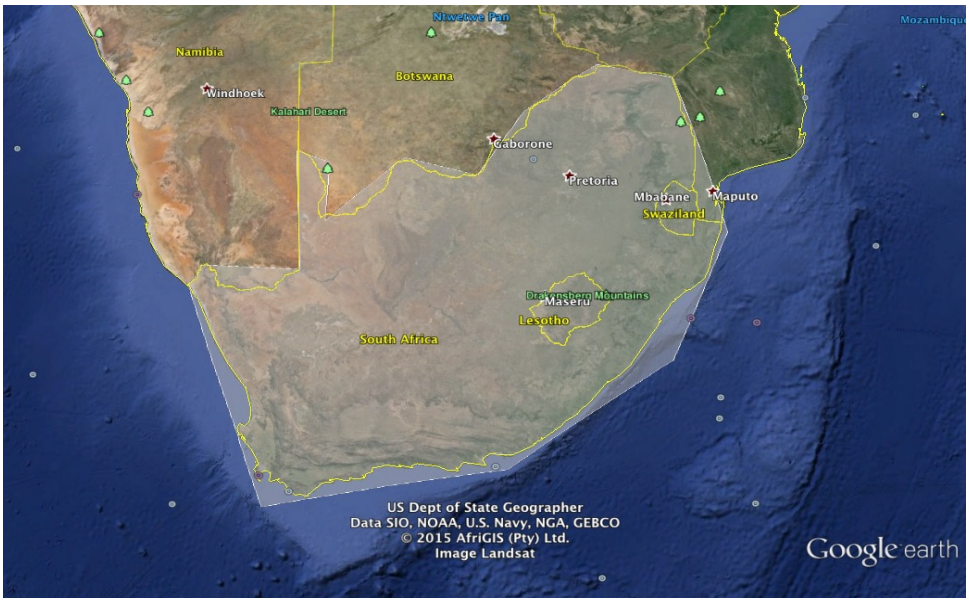

Figure 19: The South Africa validation area

Figure 19 shows the number of strokes and the strokes density at the MSG timeslots. It is important to note the increasing of both indices at the mid of the afternoon with a peak of about 2200 strokes and 16 strokes per pixel, giving an idea of the increasing of the convection.

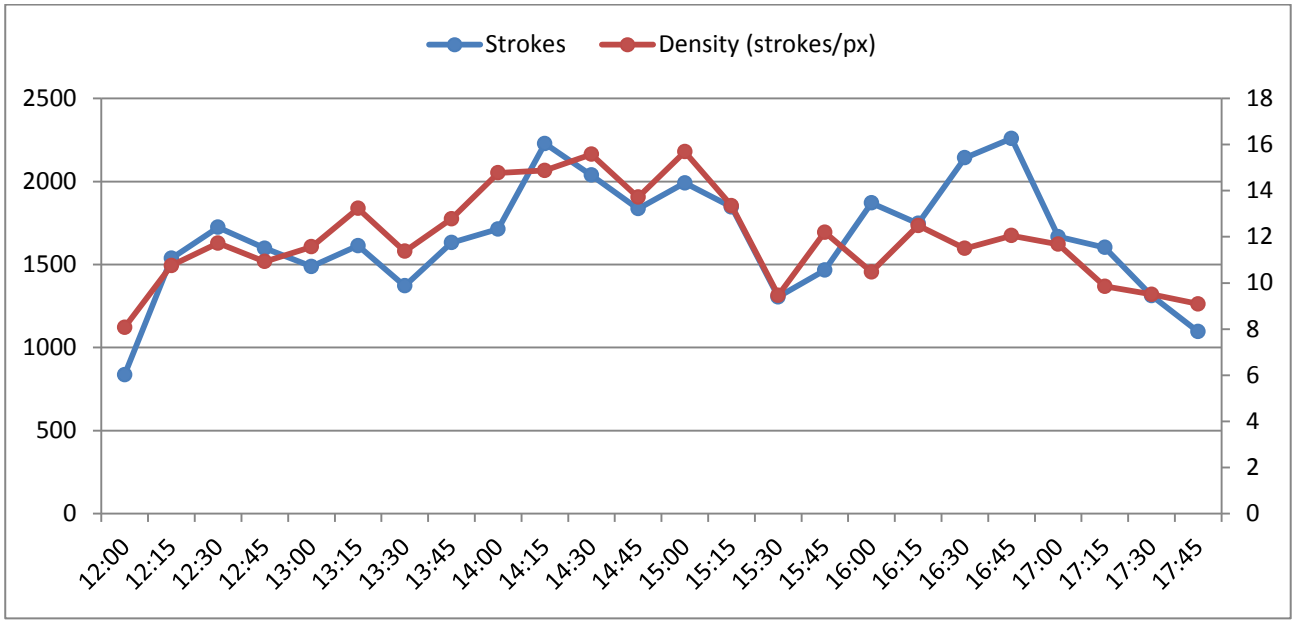

Figure 20: Number of strokes and strokes density for the event

Figure 20 shows the number of strokes per object. In this case it is important to note the increasing of the index starting from the 16:00 UTC, indicating a burst of the convection. The same peak is present in Figure 18 at 16:00 UTC. It is possible to infer that at that timeslot the convective objects are larger than the ones at the peak at 14:00 UTC (lower strokes density).

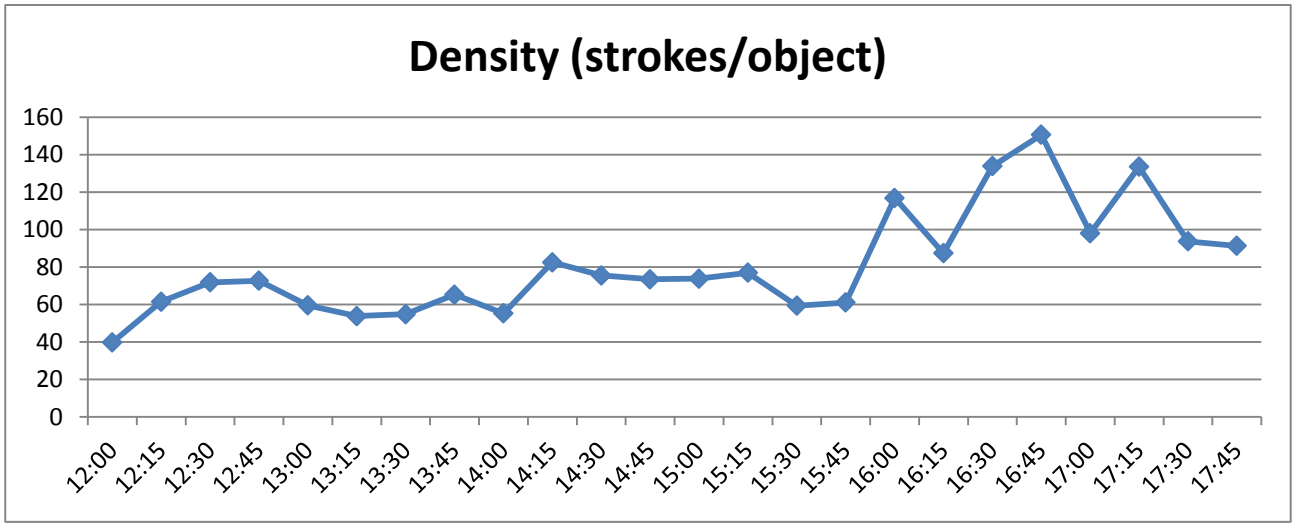

Figure 21: Strokes per objects

8.4.Results

The validation has been done using the strokes detected by the SALDN taking into account the hits 5 minutes and 5 minutes after the MSG timeslot taking into account the MSG scanning shift.

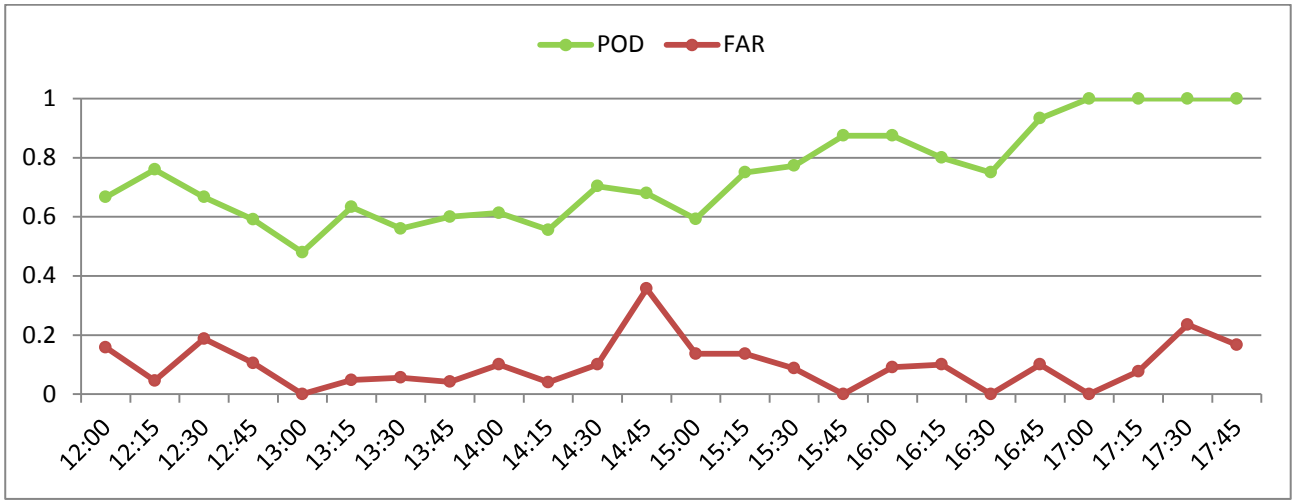

Figure 22: Performance indices of the Nefodina2 model during the whole period.

Figure 22 shows the POD and FAR scores during the time period. It is possible to note an overall very good performance of the model with a POD mean value of about 0.74 and a FAR of about 0.09. This is due to a medium-high convective activity during the whole period.

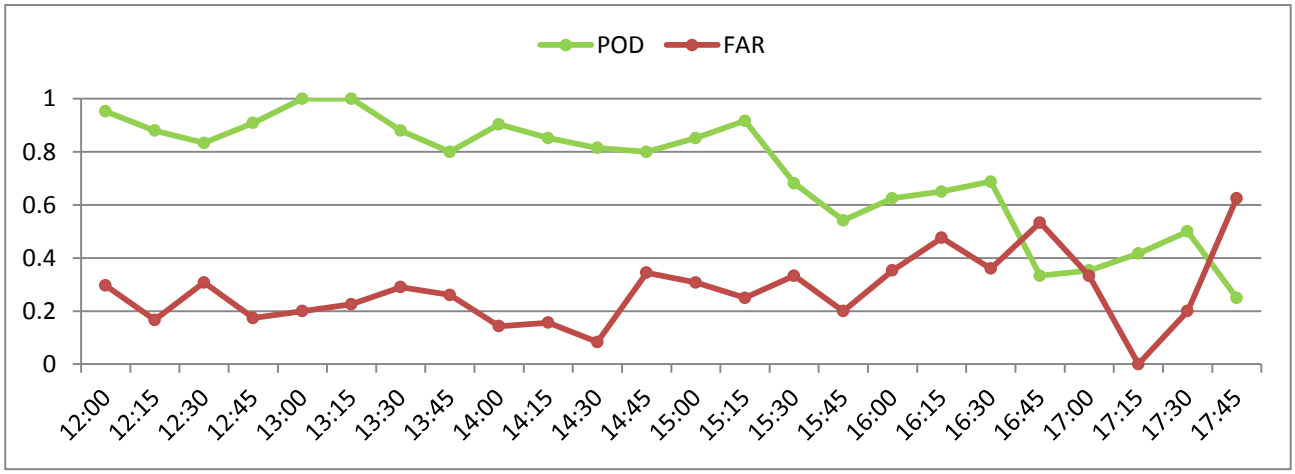

Figure 23: Performance indices of the RDT model during the whole period.

Figure 23 shows the performance indices computed for the RDT on the whole period. The graphs show a very high POD during the first part of the afternoon and a progressive decreasing of the index during the late afternoon. At the same time, the FAR increases reaching a peak of 0.6 at the end of the validation period. The mean values if the indices are 0.73 for POD and 0.27 for FAR.

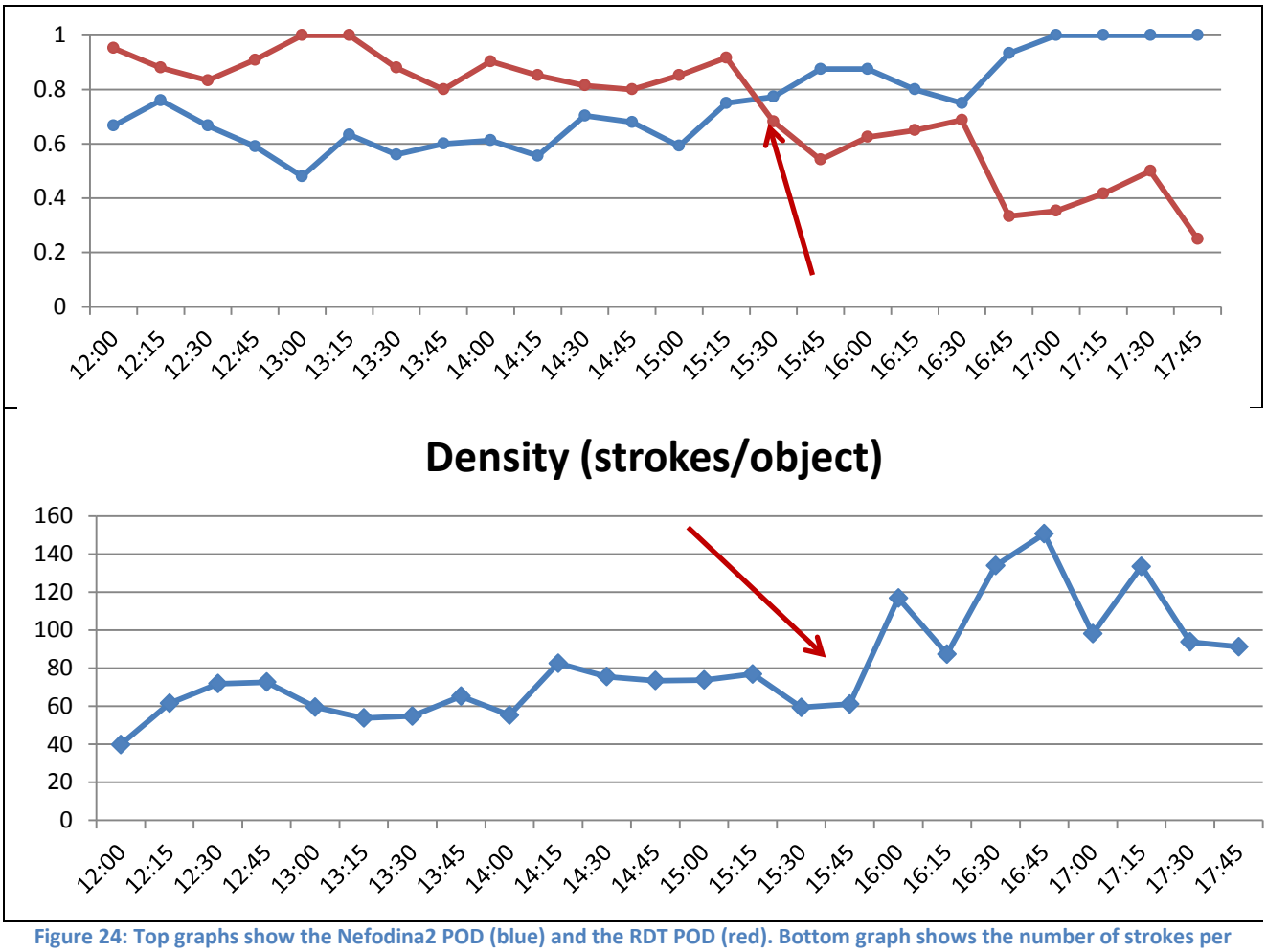

Figure 24: Top graphs show the Nefodina2 POD (blue) and the RDT POD (red). Bottom graph shows the number of strokes per object trend over the validation period.

Figure 24 shows the inversion of the Nefodina2 and RDT POD trends during the late afternoon. This happens when the density of strokes per object increases to peak at about 150 at the end of the validation period.

From these observations, it is clear that Nefodina2 is very sensitive to the strokes activity and that its performances are comparable with the RDT ones even without the use of ground data.

8.5. 16th December 2014: a weak convective case study at South Africa

This case study has been chosen in order to test the ability of the Nefodina2 model to detect weak convective objects.

The validation area is the same as the previous cast study and is shown by Figure 19.

Figure 25 shows the weather situation at 15:00 UTC. The Eastern coast of South Africa is covered with a lot of clouds which don't bring thunderstorm (stratocumulus or alto cumulus). On the Central some weak events are under development.

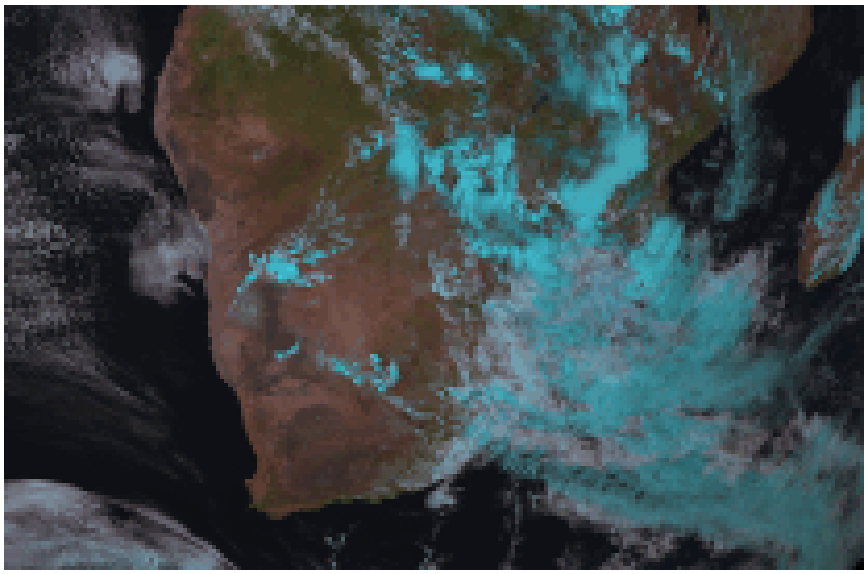

Figure 25: Meteosat RGB image at 15:00 UTC for the case study

Figure 26 shows the synoptic weather situation.

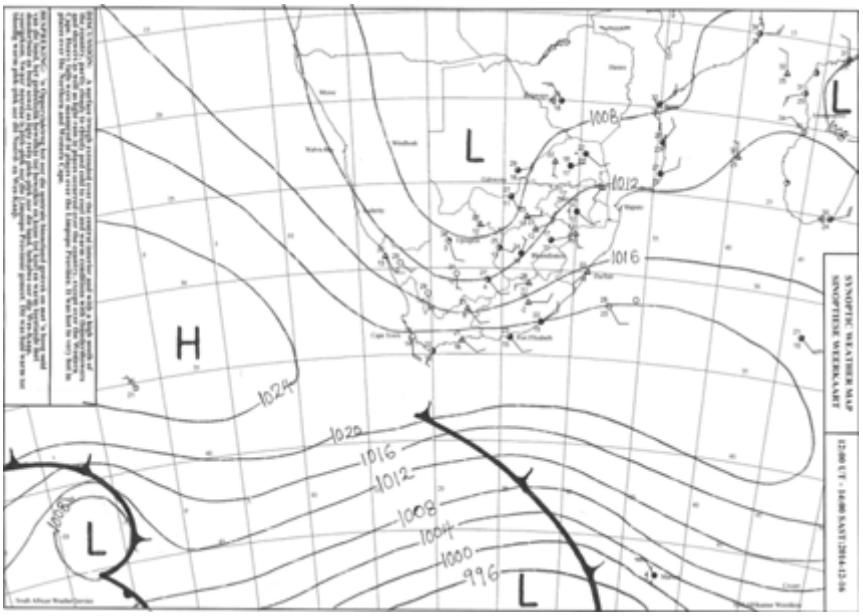

Figure 26: Synoptic chart about the case study

8.6.Event statistics

In this section some statistics about the event is presented. Figure 27 shows the number of strokes and the strokes density sampled at MSG timeslots.

The charts show a peak of about 350 cumulative strokes at 15:00 UTC which much smaller than in the previous case study (about 2000 strokes).

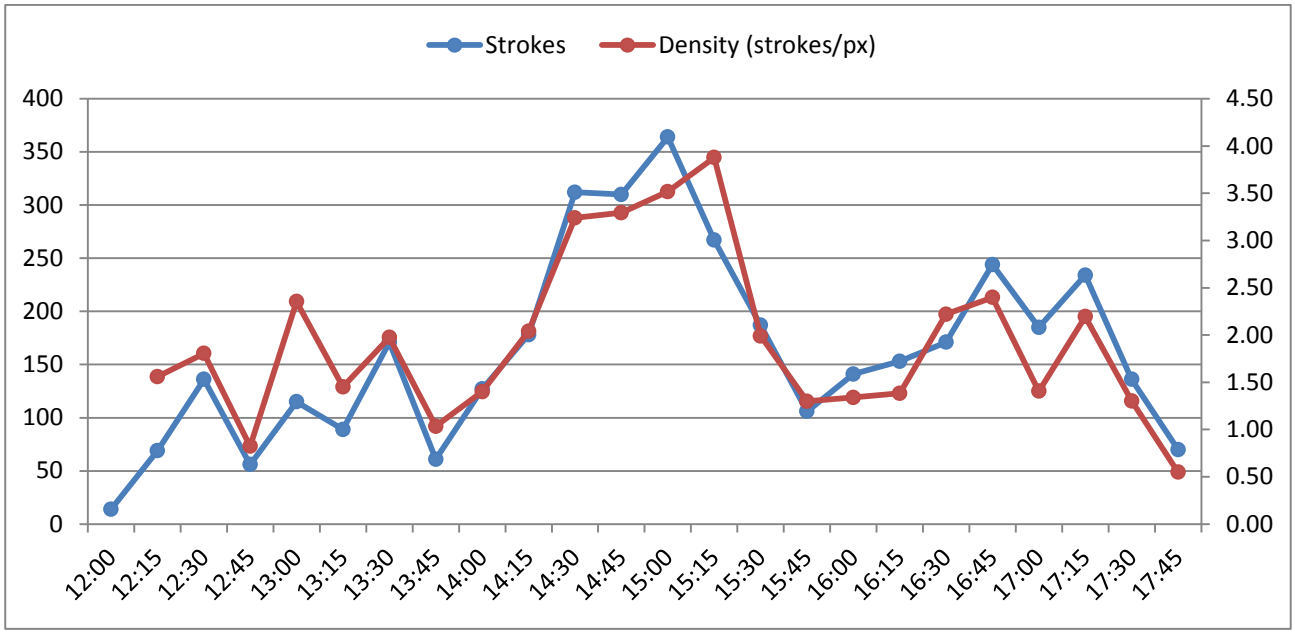

Figure 27: Number of strokes and strokes density about the case study

Figure 28 shows the number of strokes per object and again it is possible to see that the peak is below the half than the previous case study.

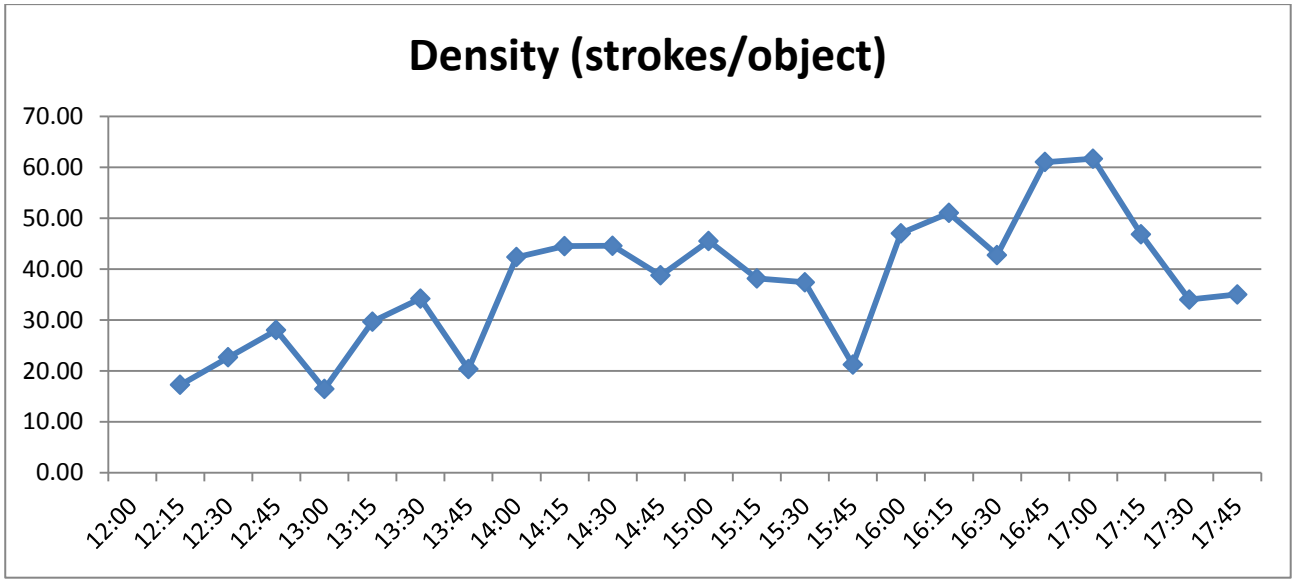

Figure 28: Strokes per convective objects about the case study

8.7.Results

The validation has been done using the strokes detected by the SALDN taking into account the hits 5 minutes and 5 minutes after the MSG timeslot taking into account the MSG scanning shift.

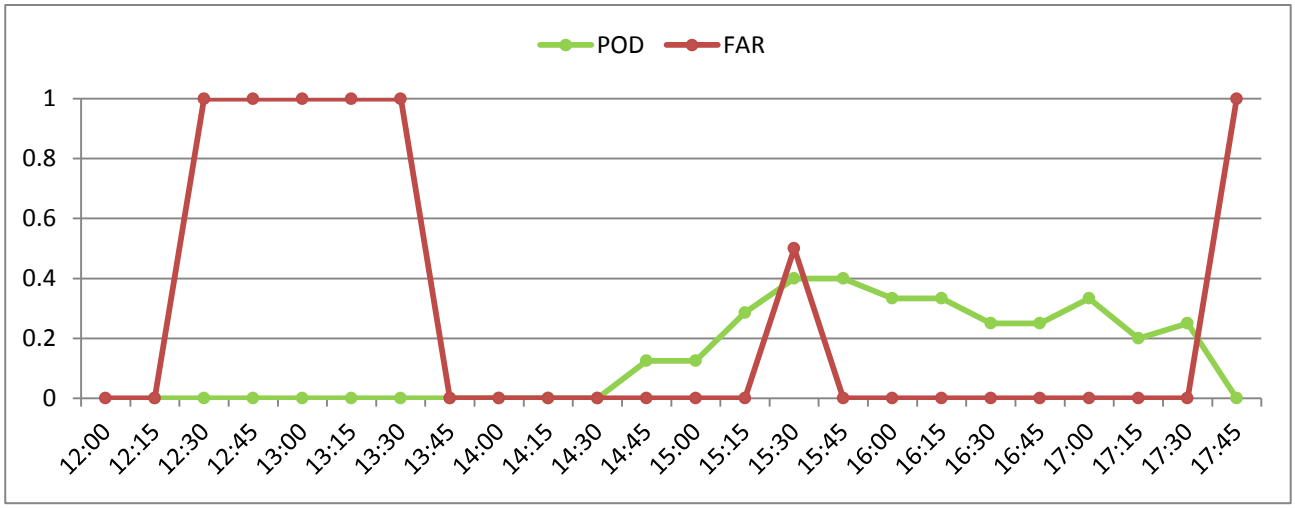

Figure 29: Nefodina2 performance indices computed for the case study

Figure 29 shows the scores of the Nefodina2 model for the case study. It is possible to note a very poor performance over the validation period. The POD score increases starting from the 14:30 UTC following the behavior of the lightning activity.

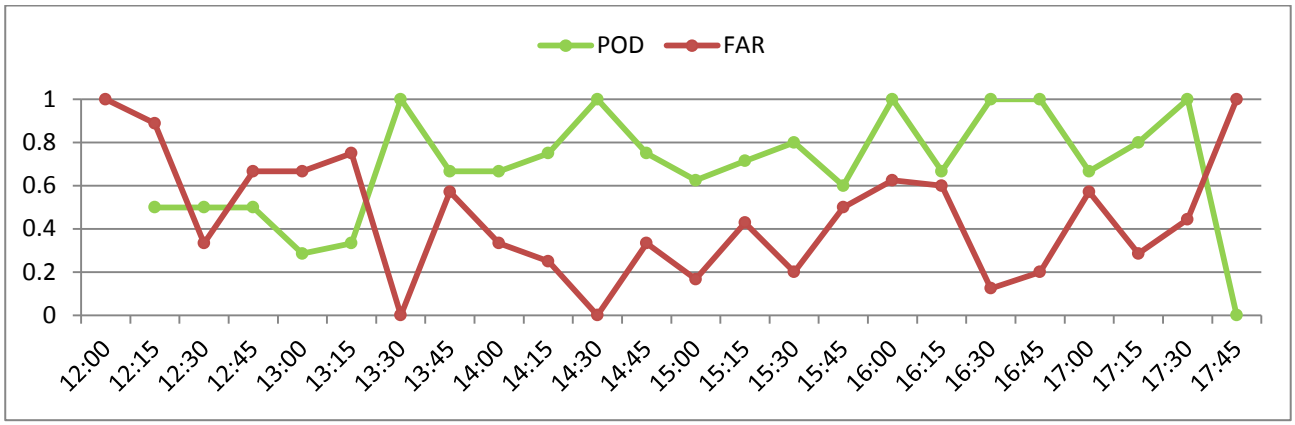

Figure 30: RDT performance indices computed for the case study

On the other side, RDT performs very well over the whole selected period. The use of the NWP data together with the lightning activity as input produces a stable and good estimation of the convective objects.

The Nefodina2 algorithm is not able to have a similar behavior because the use of the satellite images without ground data.

This case study shows that it could be interesting to evaluate the assimilation of the lightning data as input of the Nefodina2 model in order to reduce the false alarms and increases the objects detection.

9. PR-OBS-6 integration

The final goal of the study about Nefodina2 is the integration with the PR-OBS-6 HSAF product in order to have more flexibility and the extension of the product to the MSG full disk.

Figure 31 shows the actual processing flow of the PR-OBS-6 product before the integration with the Nefodina2 algorithm. It is possible to highlight the use of the MSG channel 9 and the Nowcasting SAF Cloud Type product by the current Nefodina algorithm.

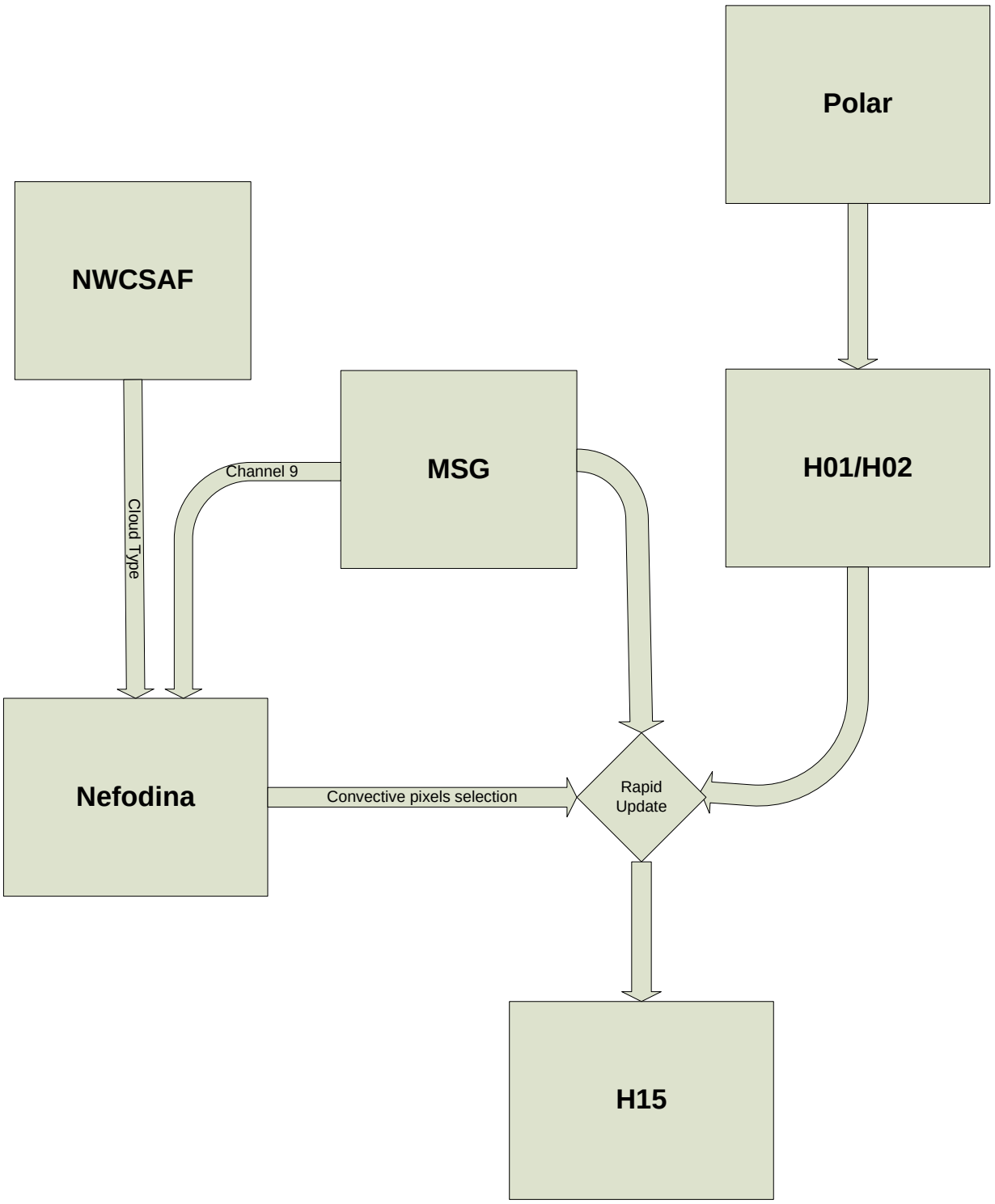

Figure 31: Current computational flow of the PR-OBS-6 product

Figure 32 shows the new computational flow after the integration with the Nefodina2 algorithm. The Meteosat channels are the 10.8 and the 6.2 and there isn't any dependency with the NWCSAF Cloud Type.

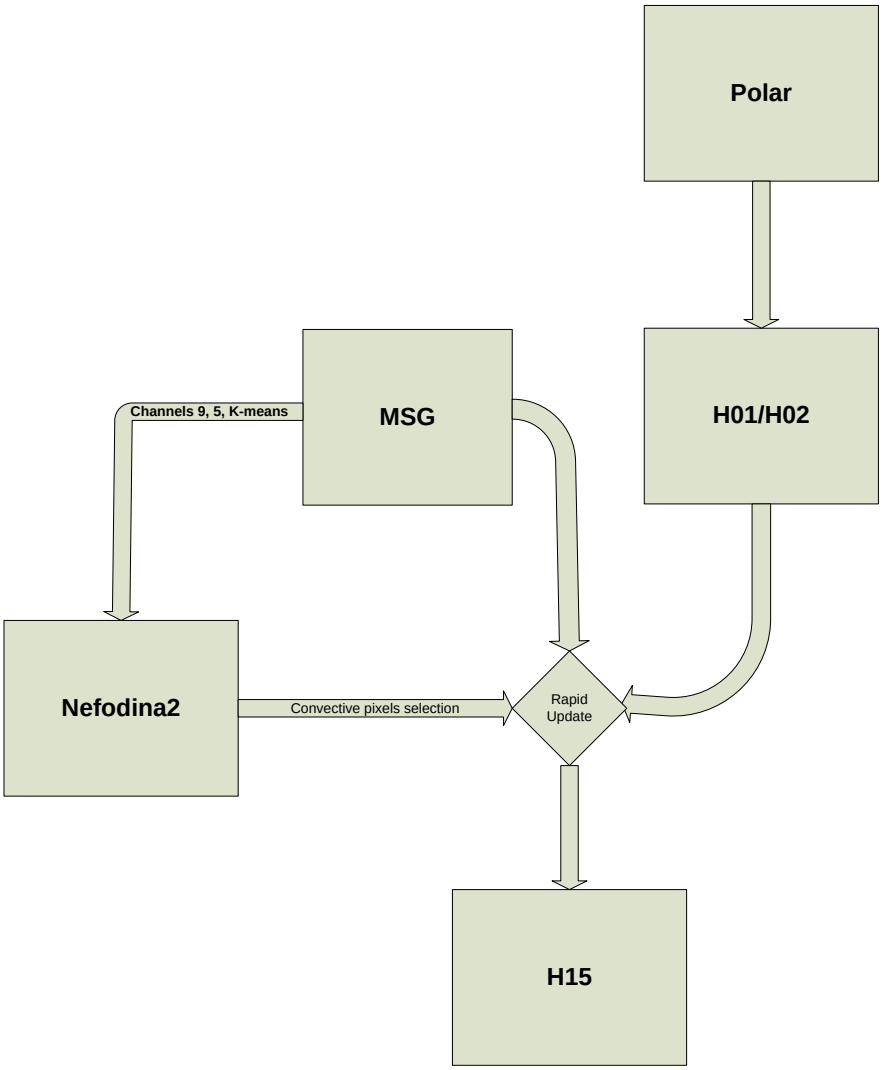

Figure 32: Actual computational flow of the PR-OBS-6 product with the Nefodina2 product

10. Summary

In this document a novel algorithm for the detection of the convective objects has been presented. The model, named Nefodina2, uses the Meteosat Second Generation images as unique data source and the channels 5, 6 and 9 in particular.

The model performances have been evaluated over some selected case studies comparing the detected objects with the lightning data using the MODE tool from the MET framework.

The Rapid Development Thunderstorms (RDT) has been chosen as benchmark in order to have a measure of the goodness of the results. The RDT model is part of the Nowcasting SAF framework for the support to the nowcasting and it is one of the most advanced thunderstorms detection and tracking model.

The indices used to access the model are the Probability of Detection (POD) and the False alarm ratio (FAR).

The use of the MODE tool has permitted to make the validation by following an objects oriented approach, given that the spatial and temporal distribution of the satellite images and the lightning data can be very different in an objective way. Moreover it has been possible to compute very standard scores following this way.

The Nefodina2 model has shown very good performances when the event under observation is heavy convective and the scores (POD and FAR) have been very similar to (sometimes better than) the RDT ones.

The Nefodina2 model depends strongly from the lightning activity and its sensitivity is less than the RDT one due to the assimilation of the NWP and lightning data.

However the model could be used for the detection and the tracking of thunderstorms under severe convective conditions. The model works on the full MSG disk and is able to work in a very flexible way having similar behaviours over different areas.

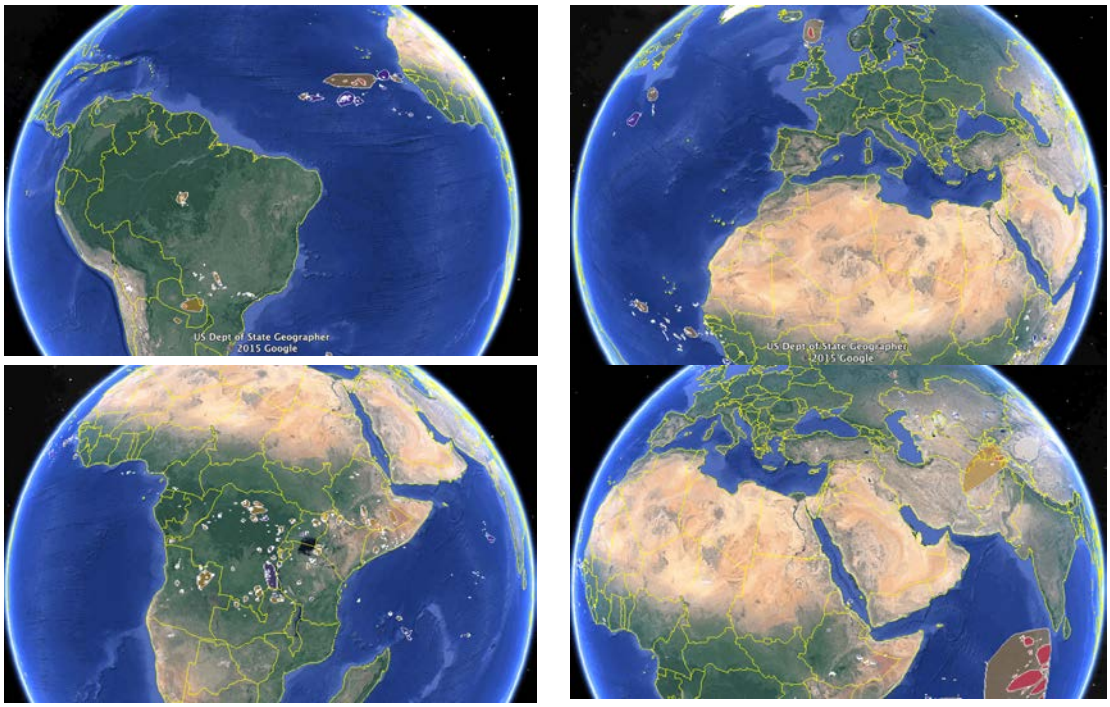

Figure 33: Parts of the full disk images produced by the Nefodina2 model.

The future developments of the model will involve the assimilation of the lightning data in order to improve the detection capabilities and reduce the number of false alarms and the parallax correction.

Moreover the use of the Rapid Scan Service at higher latitudes can be very interesting in order to increase the monitoring capability and to have a better monitoring about the fast and dangerous events.

Finally a porting over other kind of satellites like the GOES family and Himawari 8 has been planned together with the nowcasting of the detected objects.

11. Acknowledgments

South Africa Weather Service (SAWS) for the SALDN lightning data and the RDT files needed for the comparison of the two models.

Centro Nazionale di Meteorologia e Climatologia Aeronautica (CNMCA), as part of the Italian Air force, for the scientific and technical support, the MSG data and the ATDNet lightning data.

12. Bibliography

[1] An automated nowcasting system of mesoscale convective systems for the Mediterranean basin using Meteosat imagery. Part I: System description *Meteorol. Appl.* **20**: 296–307 (2013)

[2] An automated nowcasting system of mesoscale convective systems for the Mediterranean basin using Meteosat imagery. Part II: Verification statistics *Meteorol. Appl.* **20**: 296–307 (2013)

[3] Arnaud Y, Desbois M, Maizi MJ. 1992. Automatic tracking and characterization of African convective systems on Meteosat Pictures. *J. Appl. Meteorol*. **31**: 443–453.

[4] Bedka K, Brunner J, Dworak R, Feltz W, Otkin J, Greenwald T. 2010. Objective satellite-based detection of overshooting tops using infrared window channel brightness temperature gradients. *J. Appl. Meteorol. Climatol.* **49**: 181–201

[5] Feidas H, Cartalis C. 2001. Monitoring mesoscale convective cloud systems associated with heavy storms with the use of Meteosat imagery. *J. Appl. Meteorol.* **40**: 491–512

[6] Hand HW, Conway BJ. 1995. An object-oriented approach to nowcasting showers. *Weather Forecast.* **10**: 327–341.

[7] Morel C, Senesi S. 2002a. A climatology of mesoscale convective systems over Europe using satellite infrared imagery. I: methodology. *Q. J. R. Meteorol. Soc.* **128**: 1953–1971.

[8] Orlanski I. 1975. A rational subdivision of scales for atmospheric processes. *Bull. Am. Meteorol. Soc.* **56**: 527–530.

[9] Fujita T. 1981. Tornadoes and downbursts in the context of generalized planetary scales. *J. Atmos. Sci.* **38**: 1511–1534.

[10] Hodges KI, Thorncroft CN. 1997. Distribution and statistics of African mesoscale convective weather systems based on the ISCCP Meteosat imagery. *Mon. Weather Rev.* **125**: 2821–2837.

[11] Morel C, Senesi S. 2002a. A climatology of mesoscale convective systems over Europe using satellite infrared imagery. I: methodology. *Q. J. R. Meteorol. Soc.* **128**: 1953–1971.

[12] Morel C, Senesi S. 2002b. A climatology of mesoscale convective systems over Europe using satellite infrared imagery. II. Characteristics of European mesoscale convective systems. *Q. J. R. Meteorol. Soc.* **128**: 1973–1995.

[13] Roca R, Ramanathan V. 1999. Scale dependence of monsoonal convective systems over the Indian Ocean. *J. Clim.* **13**: 1286–1298.

[14] Riosalido R. 1996. Current status and principal challenges in strong convection nowcasting in COST-78 frame. Proceedings of COST-*78 International Workshop on Improvement of Nowcasting Technology*, 25–28 March, Bologna, EUR 16996 EN; 37–47.

[15] Puca S, Biron D, De Leonimbus L, Melfi D, Rosci P, Zauli F. 2005. A neural network algorithm for the nowcasting of severe convective systems. *CIMSA 2005 – IEEE International Conference on Computing Intelligence for Measurement System Applications*, 20–22 July, Giardini Naxos.

[16] Davis, C.A., B.G. Brown, and R.G. Bullock, 2006a: Object-based verification of precipitation forecasts, Part I: Methodology and application to mesoscale rain areas. *Monthly Weather Review,* **134**, 1772-1784.

[17] S. Keogh, E. Hibbett, J. Nash and J. Eyre, The Met Office Arrival Time Difference (ATD) system for thunderstorm detection and lightning location. Met Office, *Numerical Weather Prediction : Forecasting Research Technical Report No.488*

[18] J. Nash et. al, Progress in Introducing New Technology sites for the Met Office long range lightning detection system, *Paper 2.9 WMO Technical Conference on Meteorological and Environmental Instruments and Methods of Observation (TECO-2005), Instruments and Observing Methods Report No. 82*, WMO/TD-No. 1265

[19] www. cfconventions.org

[20]Gijben M. The lightning climatology of South Africa. *S Afr J Sci. 2012;* **108**(3/4) Art. #740, 10 pages.